ADVANCED ENERGY MATERIALS
www.advenergymat.de

Poly(fluorene)-Based Anion Exchange Membrane Demonstrating Excellent Durability at 1.5 A cm^{-2} for 2400 h in Water Electrolyzers

Haeryang Lim, Nam In Kim, Giwon Shin, Jaehun Lee, Sungryong Kim, Shin-Woo Myeong, Chiho Kim, Sung Mook Choi,* and Taiho Park**

Anion exchange membrane water electrolyzer (AEMWE) is a cost-effective alternative to proton exchange membrane water electrolyzer for green hydrogen production. However, AEMWE commercialization is hindered primarily by the lack of a reliable anion exchange membrane (AEM) for long-term cell durability. In this study, a poly(fluorene)-based PFAA-QA AEM is developed with a simple structure, exhibiting satisfactory OH^- conductivity (>174.6 mS cm^{-1} at 80 °C), good mechanical properties (tensile strength >35 MPa and elongation at break >51%), and excellent alkaline stability (>2000 h in 3 M KOH at 80 °C). These characteristics allow PFAA-QA-based AEMWEs to demonstrate a high cell performance (3.95 A cm^{-2} at 70 °C and 1.95 V) and long-term durability at high current densities (1.5 A cm^{-2} for 2400 h at 70 °C). Therefore, the durability of these AEMWEs surpasses that of most AEMWEs with a low voltage decay rate (>29 mV kh^{-1}).

1. Introduction

Electrochemical applications based on polymer electrolytes have garnered widespread attention as the forces driving the energy technology transition toward realizing a sustainable society with net-zero carbon emissions.[1–4] Thin polymer electrolytes reduce ohmic resistance (R_{ohm}) and enhance ion conduction, maximizing current density and energy efficiency in electrochemical devices.[5,6] Proton exchange membrane water electrolyzers (PEMWEs) have come under the spotlight as viable platforms for green hydrogen production; however, they are cost-intensive owing to the use of expensive platinum group metal (PGM) electrocatalysts and membranes.[7] Therefore, developing anion exchange membrane water electrolyzers (AEMWEs), which utilize cost-effective catalysts (such as Ni or Co), instead of expensive PGM catalysts, while exhibiting rapid oxygen evolution kinetics,[8–10] is considered an effective strategy to reduce hydrogen production costs.

However, their widespread adoption has been hindered by their low current density and long-term durability, which are inferior to those of PEMWEs.[11,12] To achieve a high AEMWE performance, the AEM must exhibit sufficient OH^- conductivity, good mechanical properties, and high alkaline stability, which are challenging to achieve.[13–15] Recent studies have reported AEMWEs, constituting AEMs with a high OH^- conductivity (>160 mS cm^{-1}), exhibiting current densities that surpass those of PEMWEs; facilitated by precisely engineered catalysts and supportive electrolytes with high alkalinity.[16–18] To achieve AEMs with good mechanical properties and high alkaline stability, researchers have engineered polymers with an aryl ether-free main chain structure, combined with cyclic or spacer-type quaternary ammonium conducting groups.[19–21] The developed AEM has shown exceptional chemical stability, maintaining over 90% of its initial OH^- conductivity for >1000 h in concentrated alkaline conditions at high temperatures (>80 °C).[18,21]

However, despite the exceptional alkaline stability of these AEMs, few AEMWEs exhibit satisfactory cell durability with minimal voltage decay, hindering commercialization. For example, Miyatake et al. developed a QTAF-3.0 AEM, which showed high OH^- conductivity, favorable mechanical properties, and exceptional alkaline stability. The corresponding AEMWE demonstrated remarkable cell durability at 1.0 A cm^{-2} and 80 °C for 1000 h.[22] Zhang et al. reported a multiblock PBPA-b-BPP AEM with excellent OH^- conductivity, outstanding mechanical durability, and exceptional alkaline stability. The corresponding AEMWE showed remarkable durability for 1250 h at 1.0 A cm^{-2} and 60 °C.[17] Wang et al. demonstrated that a tPBPp-0.6-OH AEM network with high OH^- conductivity, remarkable mechanical strength, and persistent alkaline stability. The corresponding AEMWE functioned for 430 h at 1.6 A cm^{-2} and 60 °C.[23]

H. Lim, G. Shin, S. Kim, T. Park
Department of Chemical Engineering
Pohang University of Science and Technology (POSTECH)
Pohang, Gyeongbuk 37673, Republic of Korea
E-mail: taihopark@postech.ac.kr

N. I. Kim, J. Lee, S.-W. Myeong, C. Kim, S. M. Choi
Department of Hydrogen Energy Materials, Surface & Nano Materials Division
Korea Institute of Materials Science (KIMS)
Changwon 51508, Republic of Korea
E-mail: chiho@kims.re.kr; akyzaky@kims.re.kr

S. M. Choi
Advanced Materials Engineering
University of Science and Technology (UST)
Daejeon 34113, Republic of Korea

The ORCID identification number(s) for the author(s) of this article can be found under https://doi.org/10.1002/aenm.202501038

DOI: 10.1002/aenm.202501038

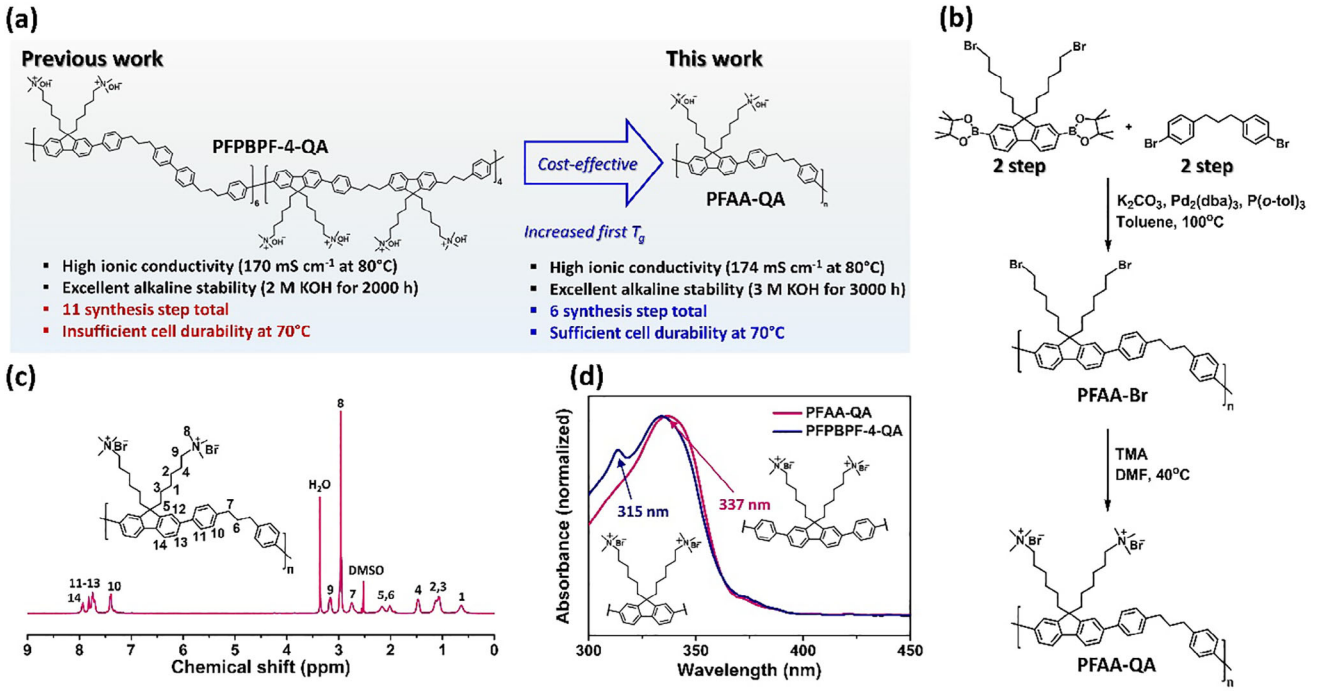

Figure 1. Structural characterization of PFAA-QA and PFPBPF-4-QA AEMs. a) Comparison of PFPBPF-4-QA and PFAA-QA. b) Synthesis of PFAA-QA AEM. c) ^{1}H NMR spectra of PFAA-QA in DMSO-d_6. d) UV–vis spectra of PFPBPF-4-QA and PFAA-QA.

Previously, we developed a PFPBPF-4-QA AEM with satisfactory OH^- conductivity, good mechanical properties, and remarkable alkaline stability.[24] Notably, the AEMWE based on PFPBPF-4-QA showed remarkable durability, with a voltage decay rate of 2 mV kh^{-1} over 800 h at 1.0 A cm^{-2} and 50 °C. The expected lifetime of prepared 1-cell AEMWE stack (active area: 63.6 cm^2) retained 90% of its initial efficiency, continuing its operation for >49 095 h. This exceptionally long operational lifetime of this AEMWE is attributed to its aryl ether-free structure and interstitial alkyl chain within the main chain. Nevertheless, despite achieving long-term stability for commercialization, the complex synthesis route and structure of PFPBPF-4-QA complex pose cost limitations. For developing commercially viable AEMWEs, the constituent AEMs must exhibit superior physicochemical properties (ion conductivity, mechanical properties, alkaline stability) and involve minimal synthesis steps to reduce production costs.[25–27]

To address these persisting challenges, in this study, we focused on developing a poly(fluorene)-based AEM with a simple structure and an interstitial alkyl chain (PFAA-QA) for AEMWEs. PFAA-QA (6 synthesis steps) requires fewer synthesis steps than does PFPBPF-4-QA (11 synthesis steps) while exhibiting superior OH^- conductivity (>174.6 mS cm^{-1} at 80 °C), excellent mechanical properties (tensile strength (TS) >35 MPa and elongation at break (EB) >51%), and exceptional alkaline stability (>2000 h in 3 M KOH at 80 °C). Herein, we elucidate the influence of the initial glass transition temperature (T_{g1}) of the fabricated AEM on the long-term durability of the corresponding electrolyzer at elevated temperatures based on a comprehensive comparison of the physicochemical properties of PFPBPF-4-QA and PFAA-QA. The PFAA-QA-based AEMWE demonstrated remarkable long-term durability with a voltage decay rate of 29 mV kh^{-1} over 2400 h at a constant current density of 1.5 A cm^{-2} and 70 °C—a performance unattainable by PFPBPF-4-QA and other reported AEMs.

2. Results and Discussion

2.1. Synthesis and Characterization of PFAA-QA AEM

Figure 1a compares the characteristics of previously reported poly(fluorene)-based PFPBPF-4-QA with those of PFAA-QA synthesized in the present study. The interstitial alkyl chain within the main chain of PFPBPF-4-QA allows the formation of ion transport channels, enhances mechanical properties and alkaline stability, and improves contact properties with the CL.[24] Homopolymer PFAA-QA with simple interstitial alkyl chains was synthesized to minimize the synthesis steps and avoid the loss of polymer uniformity due to random structures (Figure 1b). The number of synthesis steps for PFAA-QA (6 synthesis steps, including Suzuki–Miyaura coupling polymerization and Menshutkin reaction) is approximately half of that required for synthesizing PFPBPF-4-QA; the monomer's precise synthesis pathway is illustrated in Scheme S1 (Supporting Information). The chemical structures of the monomer and PFAA-Br have been confirmed by ^{1}H nuclear magnetic resonance (NMR) spectroscopy (Figures S1 and S2, Supporting Information). The individual peaks appearing in the spectrum of PFAA-Br show one-to-one correspondence with its expected chemical structure, indicating successful polymerization (Figure 1c). After quaternization, the peak at 3.29 ppm (methylene protons of bromohexyl) disappears, and a peak appears at 3.14 ppm (methylene protons

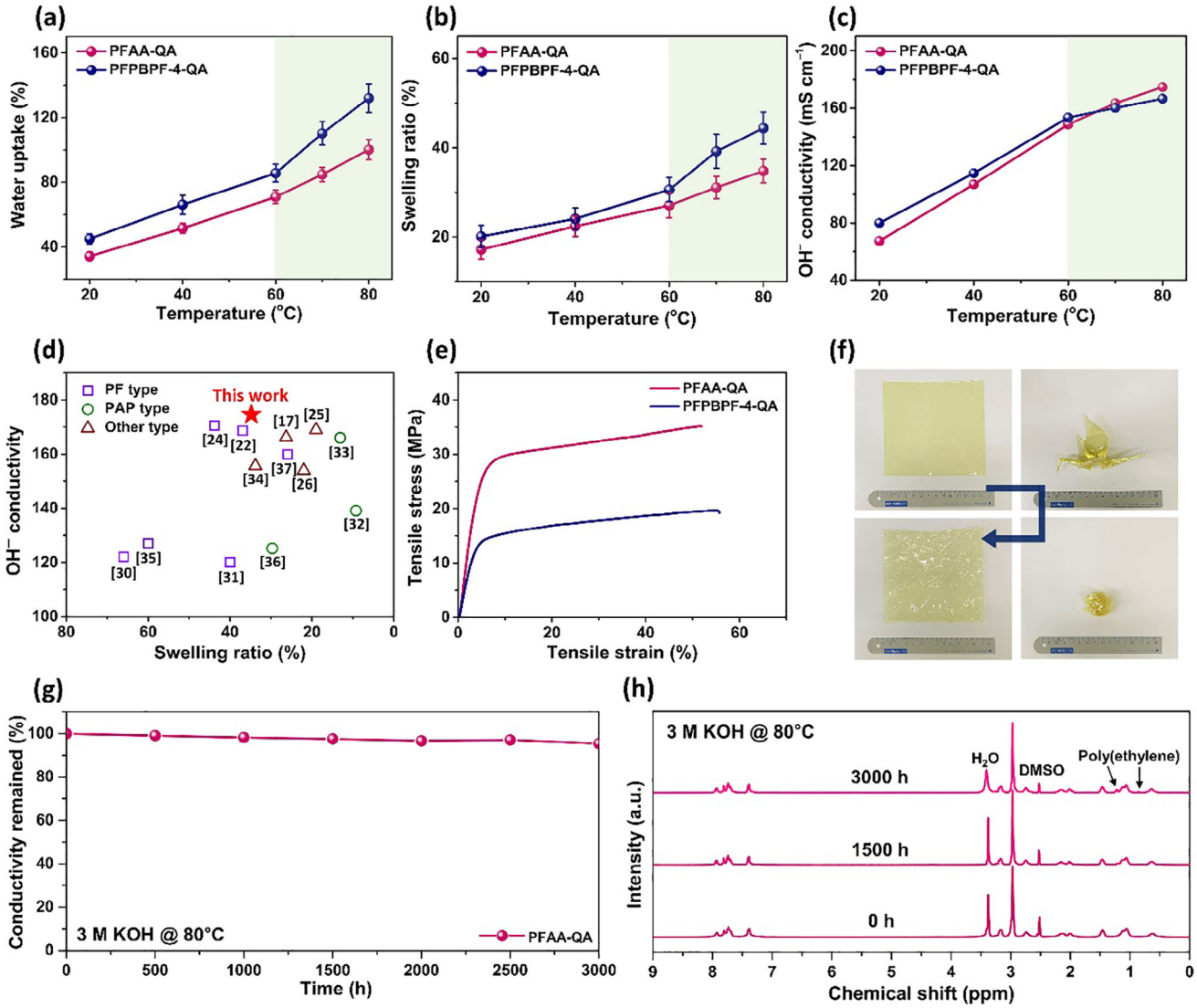

Figure 2. Physicochemical properties of PFAA-QA and PFPBPF-4-QA AEMs. a) water uptake, b) through-plane swelling ratio, and c) OH^- conductivity of PFAA-QA and PFPBPF-4-QA AEMs as functions of temperature. d) Comparison of OH^- conductivity at 80 °C with that of state-of-the-art AEMs.[17,22,24–26,30–37] e) Mechanical properties of the PFAA-QA and PFPBPF-4-QA AEMs, in OH^- form, at room temperature. f) Mechanical robustness test of PFAA-QA, in OH^- form, with size of 190 cm^2. g) OH^- conductivity retention and h) ^1H NMR spectrum of PFAA-QA after immersion in 3 M KOH at 80 °C for 3000 h.

of quaternary ammonium hexyl), indicating successful incorporation of an ion conducting group into PFAA-QA.

The configuration of PFAA-QA has been confirmed by comparing its ultraviolet–visible (UV–vis) spectra with that of PFPBPF-4-QA (Figure 1d). The UV–vis spectrum of PFPBPF-4-QA in diluted DMF solvent shows two maximum absorption peaks at 313 and 337 nm, which can be ascribed to fluorene and 2,7-diphenylfluorene moieties. Gel permeation chromatography (GPC) analysis, performed to determine the molecular weight of the intermediate polymer (PFAA-Br) before quaternization, reveals that the weight-average molecular weight and polydispersity index of PFAA-Br (76.3 kg mol^{-1} and 2.94, respectively) are slightly higher than those of PFPBPF-4-Br (64.3 kg mol^{-1} and 2.65, respectively; Figure S3 and Table S1, Supporting Information). The ^1H NMR, UV–vis, and GPC data confirm the successful synthesis of PFAA-QA. The basic properties of the PFAA-QA and PFPBPF-4-QA AEMs have been evaluated using 40 µm thick membranes fabricated by conventional solvent casting.

2.2. Comparison between the Physicochemical Properties of PFAA-QA and PFPBPF-4-QA

Figure 2a,b shows the water uptake and swelling ratio of PFAA-QA and PFPBPF-4-QA as functions of temperature (see also **Table** 1; Table S2, Supporting Information). The water uptake and swelling ratio have been measured by immersing the AEMs in water at 20–80 °C. Across the temperature range of 20–80 °C,

Table 1. IEC, water uptake, through-plain swelling ratio, OH^- conductivity, and mechanical robustness of PFAA-QA, PFPBPF-4-QA, and PiperION A40 AEMs.

Membrane code	IEC [meq g^{-1}]		Water uptake [%][b]		Swelling ratio [%][b]		OH^- conductivity [mS cm^{-1}][b]		TS [MPa]	EB [%]
	Theo	Exp[a]	20 °C	80 °C	20 °C	80 °C	20 °C	80 °C		
PFAA-QA	2.95	2.66	34.2±2.6	100.1±6.2	17.2±2.1	34.8±2.7	67.3	174.6	35.1	51.9
PFPBPF-4-QA	2.76	2.43	45.0±3.2	131.9±8.9	20.1±2.5	44.4±3.6	79.9	167.5	19.2	55.8
PiperION A40	N/A	2.37	43.1±3.1	104.4±4.7	22.5±2.9	35.1±3.2	60.2	159.5	37.7	27.5

[a] Measured by titration; [b] Measured under the fully hydrated state in OH^- form.

the water uptake and swelling ratio of PFAA-QA (water uptake: 34.2–100.1%; swelling ratio: 17.2–34.8%) are lower than those of PFPBPF-4-QA (water uptake: 45.0–131.9%; swelling ratio: 20.1–44.4%), even though the ion-exchange capacity (IEC) of the former is higher than that of the latter. As water uptake and swelling ratio typically increase with IEC,[16,28] these results are attributed to the alkyl chain ratio of PFAA-QA being lower than that of PFPBPF-4-QA. A low alkyl chain ratio suggests reduced polymer mobility, which potentially impedes ion transport channel formation, thus reducing water uptake and swelling ratio. PFAA-QA exhibits a moderate increase in both water uptake and swelling ratio with increasing temperature, whereas those of PFPBPF-4-QA drastically increase as the temperature exceeds 60 °C.

Similar to water uptake and swelling ratio, the OH^- conductivities of both PFAA-QA and PFPBPF-4-QA increase as the temperature increases to 80 °C (Figure 2c). Up to 60 °C, the OH^- conductivity of the PFPBPF-4-QA AEM remains higher than that of the PFAA-QA AEM. However, above 60 °C, the opposite trend is observed, with PFAA-QA and PFPBPF-4-QA showing OH^- conductivities of 174.6 and 166.5 mS cm^{-1}, respectively, at 80 °C. In addition, the OH^- conductivity of PFAA-QA increases proportionally to temperature, whereas that of PFPBPF-4-QA slightly increases above 60 °C because of OH^- dilution caused by the excessive water uptake and swelling ratio of PFPBPF-4-QA at certain temperatures[22,29] (these unusual temperature-dependent differences between the water uptake, swelling ratio, and OH^- conductivity of PFAA-QA and PFPBPF-4-QA are discussed later). These results indicate that the OH^- conductivity of PFAA-QA, containing interstitial alkyl chains in its polymer main chain, at 80 °C exceeds those of recently reported state-of-the-art linear type AEMs (Figure 2d).[17,22,24–26,30–37]

Mechanically stable AEMs are crucial for developing water electrolyzers with long-term durability.[34] The mechanical properties of PFAA-QA and PFPBPF-4-QA, in the OH^- form, have been evaluated at room temperature (RT) and 50% relative humidity (Figure 2e and Table 1). The TS and EB of the PFAA-QA AEM (35.1 MPa and 51.9%, respectively) are higher than those of the PFPBPF-4-QA AEM (>19.2 MPa and >55.8%, respectively). PFAA-QA, whose alkyl chain ratio in its polymer main chain is lower than that of PFPBPF-4-QA, shows reduced polymer chain mobility, thus enhancing robustness.[24] Mechanical stability tests confirm the ability of the PFAA-QA AEM (size: >190 cm^2) to withstand mechanical stress, including folding and kneading, without showing deterioration (Figure 2f). These results demonstrate the potential of the PFAA-QA AEM to withstand pressure during the fabrication of membrane electrode assemblies and cell operation.

Alkaline stability of AEM is crucial to avoid damage due to OH^- attack during water electrolyzer operation for long-term durability of cells.[38] We conducted an accelerated alkaline stability test of PFAA-QA under harsh conditions (3 M KOH solution at 80 °C) by monitoring the changes in its OH^- conductivity and chemical structure for 3000 h; this test condition is relatively harsh compared to the long-term durability conditions (1 M KOH solution at 70 °C) of AEMWEs (discussed later). PFAA-QA exhibits slightly reduced OH^- conductivity (5.4%) after the test (Figure 2g). After the alkaline stability test, no detectable changes are observed in the chemical structure of the PFAA-QA AEM (reflected by its ^1H NMR spectra), other than the leaching of poly(ethylene) caused by the usage of the HDPE bottle (Figure 2h). The integral ratio of proton in the polymer main chain and conducting groups remains unchanged, indicating the alkaline-tolerance nature of the aryl ether-free polymer main chain and spacer-type conducting groups. Thus, the slight reduction in OH^- conductivity is attributed to CO_2 poisoning of the KOH solution, which facilitates the transformation of hydroxide into carbonate or bicarbonate.[39,40]

2.3. Morphological Changes in the PFAA-QA and PFPBPF-4-QA AEMs with Temperature

To examine the anomalous temperature-dependent variations in water uptake, swelling ratio, and OH^- conductivity, we analyzed the morphological changes in PFPBPF-4-QA and PFAA-QA using atomic force microscopy (AFM). In the AFM images presented in **Figure 3**a–d, the dark regions represent clusters of hydrophilic ammonium groups and water molecules, and the bright regions indicate the hydrophobic polymer main chain.[41,42] Pristine PFAA-QA and PFPBPF-4-QA AEMs show well-developed ion transport channels with uniformly distributed hydrophilic domains of sizes 19.1 and 16.8 nm, respectively (Figure 3a,b). The large hydrophilic domain size of PFPBPF-4-QA is attributed to the high proportion of alkyl chain in its polymer main chain improving polymer mobility and facilitating aggregation of conducting groups and water molecules. We immersed both the AEMs in deionized water at 70 °C for 1 h and dried them to RT to evaluate their morphological properties (Figure 3c,d). After immersion, the hydrophilic domain size of PFAA-QA increases by ≈35% to 22.8 nm, whereas that of

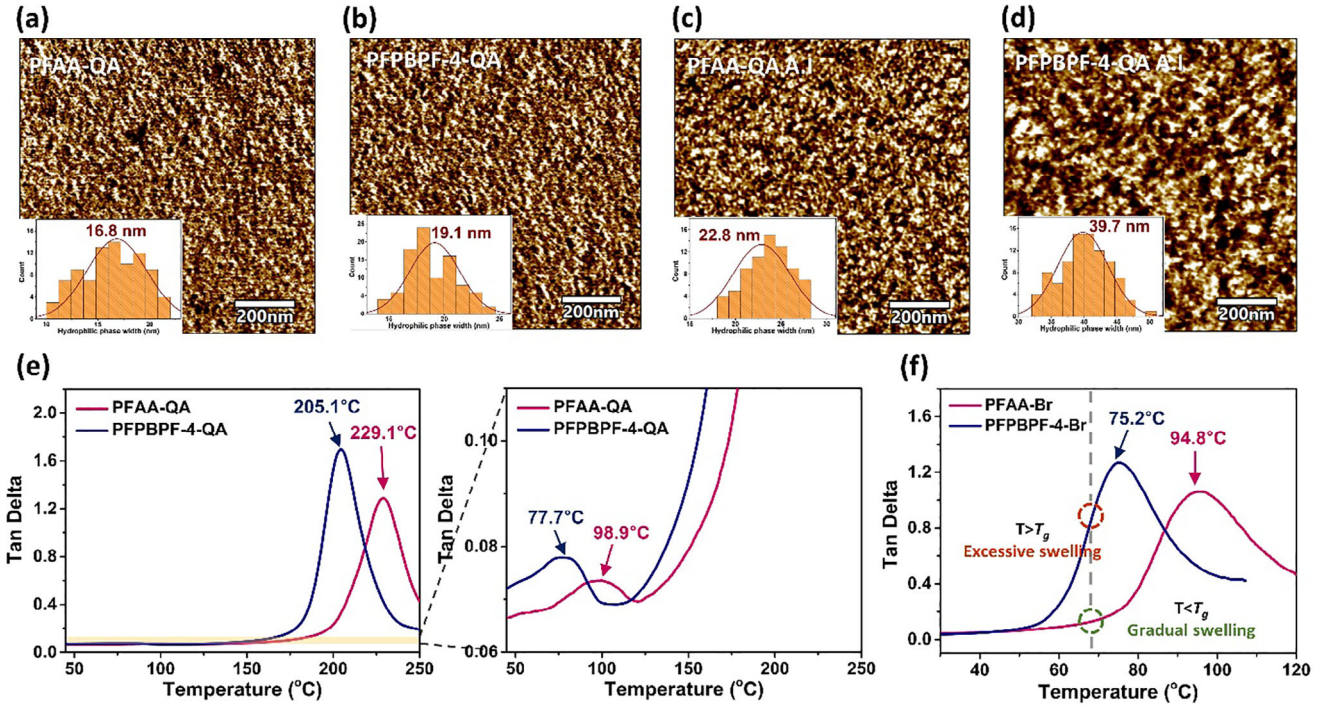

Figure 3. AFM images showing the morphologies of the membranes, in Br^- form, in dry state. a) PFAA-QA and b) PFPBPF-4-QA. c) PFAA-QA and d) PFPBPF-4-QA after immersion in water at 70 °C for 1 h. Dynamic mechanical analysis of the membranes, in Br^- form, in dry state. e) PFAA-QA and PFPBPF-4-QA. f) PFAA-Br and PFPBPF-4-Br.

PFPBPFP-4-QA drastically increases to 39.7 nm, which is more than twice that of the pristine membrane's hydrophilic domain size (Figure S4, Supporting Information). Increased mobility of PFPBPF-4-QA at certain temperatures may enhance the absorption of excess water, inducing aggregation of conducting groups and water molecules.

To elucidate the variations observed in the hydrophilic domain sizes of the two AEMs after immersion in deionized water at 70 °C, we investigated the thermal behavior of the PFPBPF and PFAA polymers within the temperature range of 40–250 °C via dynamic mechanical analysis (Figure 3e,f). PFAA-QA and PFPBPF-4-QA exhibit two relaxation peaks, T_g below 100 °C and above 200 °C. The T_{g1} (77.7 °C) and subsequent T_{g2} (205.1 °C) of PFPBPF-4-QA are lower than those of of PFAA-QA (T_{g1}: 98.9 °C; T_{g2}: 229.1 °C). The high T_g values of PFPBPF-4-QA are attributed to its high polymer mobility caused by the high proportion of alkyl chains in its polymer main chain.[24] The T_{g1} values of PFPBPF-4-QA and PFAA-QA are similar to the T_g values of PFPBPF-4-Br and PFAA-Br before quaternization as shown in Figure 3f (see also Figure S5, Supporting Information). In other words, T_{g1} and T_{g2} correspond to the hydrophobic and hydrophilic relaxation of the conducting groups, respectively.[43,44] At temperatures above 70 °C, around the T_{g1} of PFPBPF-4-QA, the mobility of the hydrophobic segment increases, resulting in excessive water absorption. Thus, after immersion at 70 °C, the hydrophilic domain size of PFPBPF-4-QA exceeds that of PFAA-QA. This result indicates that the excessive increase in water uptake and swelling ratio, and slightly increase in OH^- conductivity, of PFPBPF-4-QA (relative to those of PFAA-QA) at temperatures above 70 °C can be attributed to ion dilution.

2.4. AEMWE Single-Cell Performance

To assess the feasibility of applying PFAA-QA AEMs in practical applications, an AEMWE single cell were fabricated using a Co_3O_4 anode and Pt/C cathode in flowing 1 M KOH, which served as the anolyte (**Figure 4**a).[45] The *I–V* curves of the PFAA-QA-based AEMWE single cell at different operating temperatures are displayed in Figure 4b. The performance of the AEMWE improves upon increasing the operating temperature (50, 60, and 70 °C), and the highest current density of 3.94 A cm^{-2} is recorded at 70 °C at a cell voltage of 1.95 V. Next, electrochemical impedance spectroscopy (EIS) analysis shows that as the cell temperature increases, both R_{ohm} and the charge transfer resistance (R_{ct}) decrease owing to the enhanced OH^- conductivity and improved electrochemical properties of the catalyst with increasing temperature (Figure S6, Supporting Information).[46] For performance comparison, the AEMWE single cells were fabricated using components and methods identical to those used for the previously reported PFPBPF-4-QA and commercial PiperION A40 AEMs. In addition, the cell performances of PFPBPF-4-QA and PiperION A40 were evaluated at various operating temperatures (Figures S7 and S8, Supporting Information). Evidently, at 70 °C and a cell voltage of 1.95 V, the current density achieved by PFAA-QA (3.95 A cm^{-2}) is comparable to that of PFPBPF-4-QA (3.97 A cm^{-2}) and almost 12% higher than that of commercial PiperION A40 (3.52 A cm^{-2}) (Figure 4c). Furthermore, the EIS analysis was performed at a current density of 0.5 A cm^{-2} to examine the influence of each AEM on the interfacial resistance of the AEMWE single cell (Figure 4d). Although all the three AEMs (PFAA-QA, PFPBPF-4-QA, and PiperION A40) possess an identical

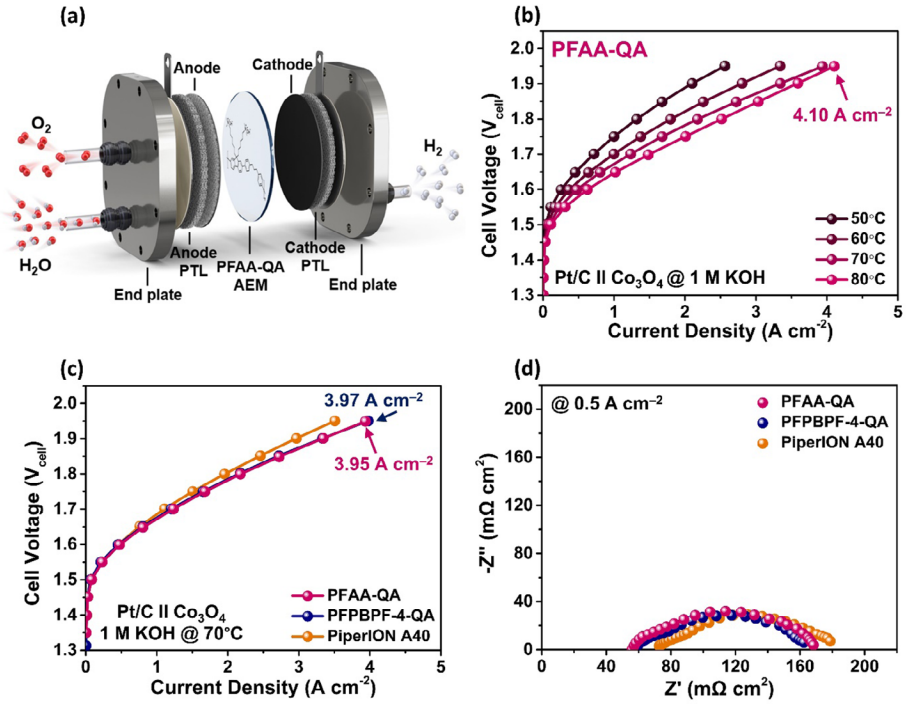

Figure 4. AEMWE single-cell investigations in 1 M KOH electrolyte using Co_3O_4 and Pt/C as the anode and cathode, respectively. a) Schematic of the AEMWE single-cell assembly. b) I–V curves of the PFAA-QA-based single cell at different temperatures. c) Comparison of cell performance and d) Nyquist plots of the AEMWE single cells based on the PFAA-QA, PFPBPF-4-QA, and commercial PiperION A40 AEMs at 70 °C in 1 M KOH.

thickness of 40 μm, the R_{ohm} values of PFAA-QA (56.1 Ω cm^2) and PFPBPF-4-QA (58.3 Ω cm^2) are lower than that of PiperION A40 (72.3 Ω cm^2). Given that R_{ohm} is primarily affected by membrane thickness and contact properties with the CL, these reduced R_{ohm} values of PFAA-QA and PFPBPF-4-QA are attributed to the interstitial alkyl chains in the conducting groups and the ability of the main chain to promote contact with the CL; these results are consistent with those reported in previous studies.[24,37] In contrast, the AEMWE single cells based on the these three AEMs (PFAA-QA, PFPBPF-4-QA, and PiperION A40) exhibit comparable values of R_{ct}, which is predominantly influenced by the electrocatalytic properties of the anode and cathode rather than those of the membrane.[47]

2.5. AEMWE Single-Cell Durability

Realizing consistent long-term durability under high current density is crucial for AEMWE commercialization. To maintain stable operation at high current densities, decreasing the cell voltage is imperative. Thus, operating the cell at elevated temperatures is necessary to mitigate damage to the membrane and catalyst from high cell voltage.[48] The durability of the PFAA-QA-based AEMWE was evaluated at a constant current density of 1.0 A cm^{-2} for 100 and 50 h at 50 and 70 °C, respectively, and compared with that of the PFPBPF-4-QA-based cell under the same conditions as shown in **Figure 5a** (see also Figure S9, Supporting Information). Both the PFAA-QA and PFPBPF-4-QA AEMs demonstrate stable cell voltages with negligible voltage decay rates at a constant current density of 1.0 A cm^{-2} and temperature of 50 °C for 100 h. This result aligns with the outstanding cell durability of previously reported PFPBPF-4-QA, which enables a voltage decay rate of 2 mV kh^{-1} under the same conditions.[24] However, at 70 °C, PFPBPF-4-QA shows rapid cell degradation, whereas PFAA-QA exhibits remarkable durability, due to T_{g1} of the former being lower than that of the latter as discussed before (Figures 2b and 5b). At a temperature close to T_{g1}, the dynamic motion of the polymer chain drastically modifies the physical properties of PFPBPF-4-QA, thereby compromising the membrane's mechanical properties. Consequently, the AEMWE cell rapidly degrades, even though chemical degradation does not occur (Figure S10, Supporting Information). The PFAA-QA-based AEMWE single cell demonstrated the capability to operate at 2.0 A cm^{-2} and 80 °C (Figure S11, Supporting Information). However, it was considered challenging to sustain operation for thousands of hours due to the temperature overlapping with PFAA-QA's T_{g1} and the power supply's incapacity to consistently cover the 4.9 cm^2 active area.

To further confirm the high durability performance of PFAA-QA, a long-term durability test was conducted for 2400 h under a constant current density of 1.5 A cm^{-2} at 70 °C in a 1 M KOH solution (Figure 5c). The PFAA-QA-based AEMWE exhibits excellent cell durability with a voltage decay rate of 29 mV kh^{-1} for 2400 h. The initial cell efficiency is ≈77.9%, and after the 2400 h test, the measured final efficiency is ≈74.7%, reflecting an efficiency loss of only 3.2%. During the initial 1000 h of operation, the cell voltage increases slightly, showing a decay rate of 56 mV kh^{-1}, due to changes in the interface structure of the catalyst or ionomer.[49] After the initial stabilization, the cell voltage remains stable with a minimal voltage decay rate of 14 mV kh^{-1} during

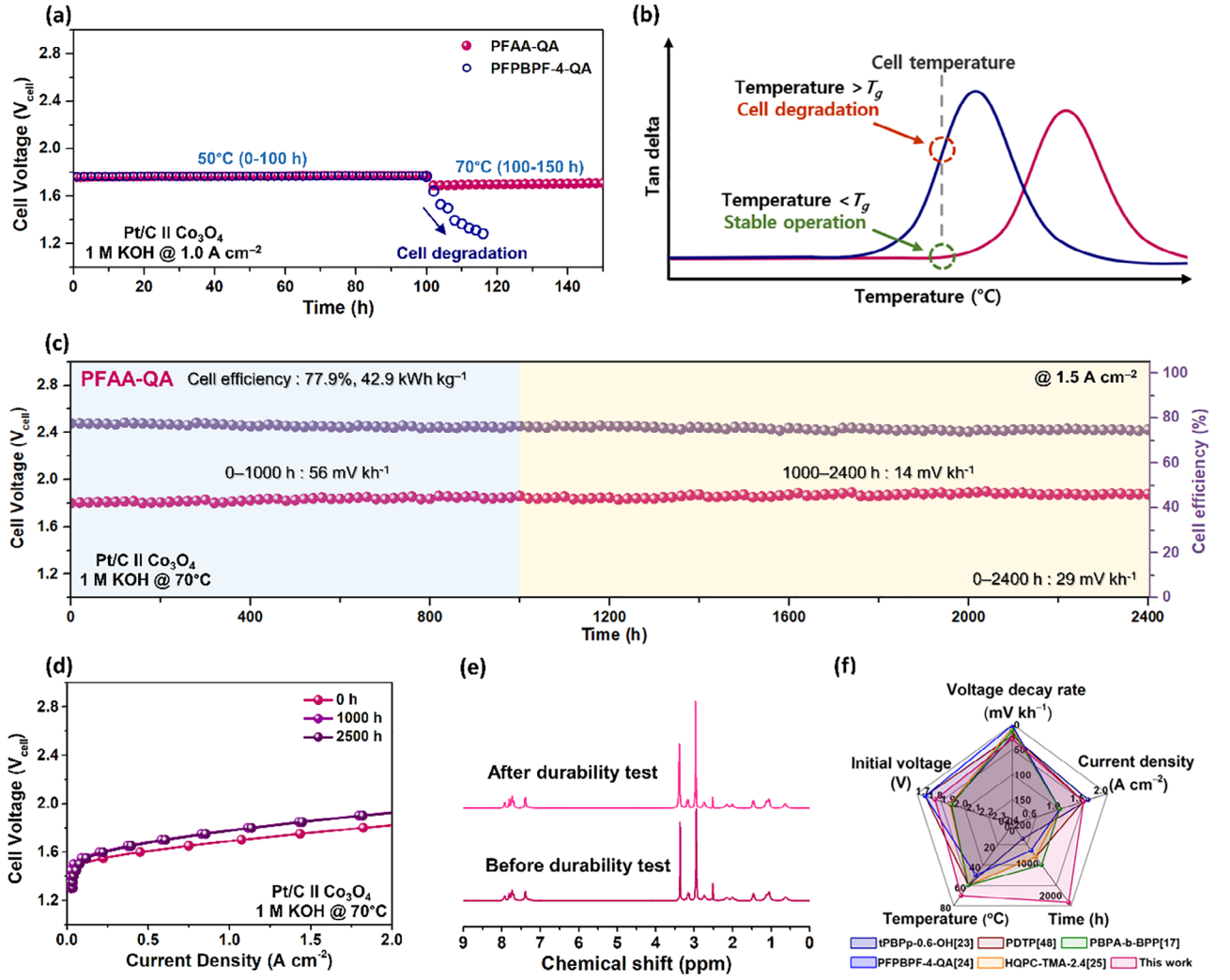

Figure 5. AEMWE durability test in the single cell condition. a) Durability analysis of PFAA-QA and PFPBPF-4-QA under a current density of 1.0 A cm^{-2} at two different temperatures, 50 and 70 °C. b) Illustration of the impact of the AEM's initial T_g on cell degradation. c) Long-term durability test of PFAA-QA under a current density of 1.5 A cm^{-2} at 70 °C in 1 M KOH. d) Polarization curves of PFAA-QA during the long-term durability test. e) ^{1}H NMR spectra of PFAA-QA before and after the durability test. f) Comparison of the performance of PFAA-QA with those of other state-of-art AEMs.[17,23,24,25,50]

the subsequent 1400 h operation. No significant difference is observed between the *I*–*V* curves obtained after 1000 and 2000 h of operation during the long-term durability test (Figure 5d). After the long-term durability test, the chemical structure of PFAA-QA is confirmed and compared with its initial structure using ^{1}H NMR spectroscopy (Figure 5e). Evidently, despite the extreme operational conditions of the AEMWE, the membrane's chemical structure does not show substantial changes. The PFAA-QA AEM demonstrates superior durability under these conditions (1.5 A cm^{-2} at 70 °C in 1 M KOH). The durability of PFAA-QA in the water electrolyzer surpasses that of previously reported state-of-the-art membranes as shown in Figure 5f (see also Figure S12, Supporting Information).[17,23,24,25,50]

3. Conclusion

In summary, we developed a poly(fluorene)-based PFAA-QA AEM with a simple structure as an improved alternative to our previously constructed PFPBPF-4-QA AEM. PFAA-QA, with a suitable T_{g1}, exhibited satisfactory OH^- conductivity, sufficiently good mechanical properties, and excellent alkaline stability, enhancing the performance and long-term durability of the corresponding AEMWE cell. Owing to these properties, the PFAA-QA-based AEMWE single cell achieved a remarkable current density of 3.95 A cm^{-2} at 1.95 V and 70 °C, outperforming the commercial benchmark PiperION A40 (3.52 A cm^{-2} at 1.95 V) despite utilizing a PGM-free anode. Additionally, the prepared cell demonstrated long-term durability with a reliable voltage decay rate of 29 mV kh^{-1} under a high current density of 1.5 A cm^{-2} at 70 °C for 2400 h. These values surpass those achieved by previously reported PFPBPF-4-QA and other AEMs. The efficient poly(fluorene)-based PFAA-QA AEM synthesized in this study is expected to facilitate practical water electrolysis, zero-gap CO_2 reduction reactions, and other electrochemical applications.

Supporting Information

Supporting Information is available from the Wiley Online Library or from the author.

Acknowledgements

H.L. and N.I.K. contributed equally to this work. This work was supported by National Research Foundation of Korea (NRF) grants funded by the Ministry of Science and ICT (MSIT) (Nos. 2021R1A5A1084921, RS-2024-00467234) and the Fundamental Research Program of the Korean Institute of Materials Science (PNKA200) in the Republic of Korea. Part of this work was also supported by Basic Science Research Program through the National Research Foundation of Korea(NRF) funded by the Ministry of Education (RS-2024-00410756).

Conflict of Interest

The authors declare no conflict of interest.

Data Availability Statement

The data that support the findings of this study are available from the corresponding author upon reasonable request.

Keywords

anion exchange membrane, glass transition temperature, long-term durability, PGM-free catalysts, water electrolyzer

Received: February 22, 2025
Revised: April 14, 2025
Published online: May 2, 2025

[1] B. Endrődi, E. Kecsenovity, A. Samu, T. Halmágyi, S. Rojas-Carbonell, L. Wang, Y. Yan, C. Janáky, *Energy Environ. Sci.* **2020**, *13*, 4098.
[2] H. Zhou, F. Yu, Q. Zhu, J. Sun, F. Qin, L. Yu, J. Bao, Y. Yu, S. Chen, Z. Ren, *Energy Environ. Sci.* **2018**, *11*, 2858.
[3] S. Choi, S.-H. Shin, D.-H. Lee, G. Doo, D. W. Lee, J. Hyun, J. Y. Lee, H.-T. Kim, *J. Mater. Chem. A* **2022**, *10*, 789.
[4] Z. Qiao, J. Deng, T. Chen, *Macromol. Res.* **2023**, *32*, 145.
[5] R. Phillips, A. Edwards, B. Rome, D. R. Jones, C. W. Dunnill, *Int. J. Hydrogen Energy* **2017**, *42*, 23986.
[6] T. J. Omasta, L. Wang, X. Peng, C. A. Lewis, J. R. Varcoe, W. E. Mustain, *J. Power Sources* **2018**, *375*, 205.
[7] S. M. Saba, M. Müller, M. Robinius, D. Stolten, *Int. J. Hydrogen Energy* **2018**, *43*, 1209.
[8] P. Chen, X. Hu, *Adv. Energy Mater.* **2020**, *10*, 2002285.
[9] P. Thangavel, H. Lee, T. H. Kong, S. Kwon, A. Tayyebi, J. h. Lee, S. M. Choi, Y. Kwon, *Adv. Energy Mater.* **2022**, *13*, 2203401.
[10] P. Shirvanian, A. Loh, S. Sluijter, X. Li, *Electrochem. Commun.* **2021**, *132*, 107140.
[11] J. Pan, C. Chen, Y. Li, L. Wang, L. Tan, G. Li, X. Tang, L. Xiao, J. Lu, L. Zhuang, *Energy Environ. Sci.* **2014**, *7*, 354.
[12] X. Peng, D. Kulkarni, Y. Huang, T. J. Omasta, B. Ng, Y. Zheng, L. Wang, J. M. LaManna, D. S. Hussey, J. R. Varcoe, I. V. Zenyuk, W. E. Mustain, *Nat. Commun.* **2020**, *11*, 3561.
[13] G. Merle, M. Wessling, K. Nijmeijer, *J. Membr. Sci.* **2011**, *377*, 1.
[14] F. Xu, Y. Chen, B. Lin, J. Li, K. Qiu, J. Ding, *ACS Macro Lett.* **2021**, *10*, 1180.
[15] X. Wu, N. Chen, H. A. Klok, Y. M. Lee, X. Hu, *Angew. Chem., Int. Ed. Engl.* **2022**, *61*, 202114892.
[16] N. Chen, S. Y. Paek, J. Y. Lee, J. H. Park, S. Y. Lee, Y. M. Lee, *Energy Environ. Sci.* **2021**, *14*, 6338.
[17] Y. Ma, C. Hu, G. Yi, Z. Jiang, X. Su, Q. Liu, J. Y. Lee, S. Y. Lee, Y. M. Lee, Q. Zhang, *Angew. Chem., Int. Ed. Engl.* **2023**, *62*, 202311509.
[18] T. Tang, H. Lee, Z. Wang, Z. Li, L. Wang, D. Chen, W. Zheng, Q. Liu, L. He, G. Ding, Z. Tian, L. Sun, *Energy Environ. Sci.* **2024**, *17*, 7816.
[19] H. Lim, I. Jeong, J. Choi, G. Shin, J. Kim, T.-H. Kim, T. Park, *Appl. Surf. Sci.* **2023**, *610*, 155601.
[20] J. Choi, Y. Lee, H. Lim, H. Maeng, T. Park, T.-H. Kim, *ACS Appl. Polym. Mater.* **2024**, *6*, 11291.
[21] W. Yuan, L. Zeng, S. Jiang, C. Yuan, Q. He, J. Wang, Q. Liao, Z. Wei, *J. Membr. Sci.* **2022**, *657*, 120676.
[22] F. Liu, K. Miyatake, A. M. A. Mahmoud, V. Yadav, F. Xian, L. Guo, C. Y. Wong, T. Iwataki, Y. Shirase, K. Kakinuma, M. Uchida, *Adv. Energy Mater.* **2024**.
[23] G. Deng, Y. Liao, Y. Lin, L. Ding, H. Wang, *Angew. Chem., Int. Ed. Engl.* **2024**, *63*, 202412632.
[24] H. Lim, J. Y. Jeong, G. Shin, C. Kim, G. Choi, S. W. Myeong, S. M. Choi, T. Park, *Adv. Energy Mater.* **2024**, *14*, 2401725.
[25] S. Kim, S. H. Yang, S.-H. Shin, H. J. Cho, J. K. Jang, T. H. Kim, S.-G. Oh, T.-H. Kim, H. Han, J. Y. Lee, *Energy Environ. Sci.* **2024**, *17*, 5399.
[26] M. S. Cha, J. E. Park, S. Kim, S.-H. Han, S.-H. Shin, S. H. Yang, T.-H. Kim, D. M. Yu, S. So, Y. T. Hong, S. J. Yoon, S.-G. Oh, S. Y. Kang, O.-H. Kim, H. S. Park, B. Bae, Y.-E. Sung, Y.-H. Cho, J. Y. Lee, *Energy Environ. Sci.* **2020**, *13*, 3633.
[27] J. Wang, Y. Zhao, B. P. Setzler, S. Rojas-Carbonell, C. Ben Yehuda, A. Amel, M. Page, L. Wang, K. Hu, L. Shi, S. Gottesfeld, B. Xu, Y. Yan, *Nat. Energy* **2019**, *4*, 392.
[28] J. Han, L. Zhu, J. Pan, T. J. Zimudzi, Y. Wang, Y. Peng, M. A. Hickner, L. Zhuang, *Macromolecules* **2017**, *50*, 3323.
[29] M. Zhang, H. K. Kim, E. Chalkova, F. Mark, S. N. Lvov, T. C. M. Chung, *Macromolecules* **2011**, *44*, 5937.
[30] W. H. Lee, E. J. Park, J. Han, D. W. Shin, Y. S. Kim, C. Bae, *ACS Macro Lett.* **2017**, *6*, 566.
[31] W. H. Lee, Y. S. Kim, C. Bae, *ACS Macro Lett.* **2015**, *4*, 814.
[32] M. Zeng, X. He, J. Wen, G. Zhang, H. Zhang, H. Feng, Y. Qian, M. Li, *Adv. Mater.* **2023**, *35*, 2306675.
[33] X. Wu, N. Chen, C. Hu, H. A. Klok, Y. M. Lee, X. Hu, *Adv. Mater.* **2023**, *35*, 2210432.
[34] Y. Ma, L. Li, X. You, H. Lin, G. Yi, X. Su, A. Zhu, Q. Liu, Q. Zhang, *Chem. Eng. J.* **2024**, *480*, 148225.
[35] S. Maurya, S. Noh, I. Matanovic, E. J. Park, C. Narvaez Villarrubia, U. Martinez, J. Han, C. Bae, Y. S. Kim, *Energy Environ. Sci.* **2018**, *11*, 3283.
[36] L. Liu, L. Bai, Z. Liu, S. Miao, J. Pan, L. Shen, Y. Shi, N. Li, *J. Membr. Sci.* **2023**, *665*, 121135.
[37] H. Lim, G. H. Han, D. H. Lee, G. Shin, J. Choi, S. H. Ahn, T. Park, *Small* **2024**, *20*, 2400031.
[38] Y. Lee, K. Min, J. Choi, G. Choi, H. Kim, T.-H. Kim, *J. Mater. Chem. A* **2023**, *11*, 25008.
[39] T. D. Myles, K. N. Grew, A. A. Peracchio, W. K. S. Chiu, *J. Power Sources* **2015**, *296*, 225.
[40] M. A. Hickner, A. M. Herring, E. B. Coughlin, *J. Polym. Sci., Part B: Polym. Phys.* **2013**, *51*, 1727.
[41] J. Zhang, K. Zhang, X. Liang, W. Yu, X. Ge, M. A. Shehzad, Z. Ge, Z. Yang, L. Wu, T. Xu, *J. Mater. Chem. A* **2021**, *9*, 327.
[42] H. Lim, J.-Y. Jeong, D. H. Lee, S.-W. Myeong, G. Shin, D. Choi, W. B. Kim, S. M. Choi, T. Park, *J. Mater. Chem. A* **2023**, *11*, 25938.
[43] H.-D. Nguyen, T. K. L. Nguyen, E. Planes, J. Jestin, L. Porcar, S. Lyonnard, C. Iojoiu, *J. Phys. Chem. C* **2020**, *124*, 13071.
[44] L. Assumma, C. Iojoiu, R. Mercier, S. Lyonnard, H. D. Nguyen, E. Planes, *J. Polym. Sci., Part A:Polym. Chem.* **2015**, *53*, 1941.

[45] S.-W. Myeong, J. Jeong, J.-y. Jeong, H. Lee, S. Jin, J.-H. Lee, J. Yang, J. M. Lee, Y. Kim, C. Kim, S. M. Choi, *Appl. Energy* **2024**, *371*, 123650.
[46] N. I. Kim, J. Lee, S. Jin, J. Park, J. Y. Jeong, J. Lee, Y. Kim, C. Kim, S. M. Choi, *Small Methods* **2024**, *8*, 2400284.
[47] M. J. Jang, S. H. Yang, M. G. Park, J. Jeong, M. S. Cha, S.-H. Shin, K. H. Lee, Z. Bai, Z. Chen, J. Y. Lee, S. M. Choi, *ACS Energy Lett.* **2022**, *7*, 2576.
[48] J. Lee, H. Jung, Y. S. Park, S. Woo, J. Yang, M. J. Jang, J. Jeong, N. Kwon, B. Lim, J. W. Han, S. M. Choi, *Small* **2021**, *17*, 2100639.
[49] F. Liu, K. Miyatake, M. Tanabe, A. M. A. Mahmoud, V. Yadav, L. Guo, C. Y. Wong, F. Xian, T. Iwataki, M. Uchida, K. Kakinuma, *Adv. Sci.* **2024**, *11*, 2402969.
[50] M.-G. Kim, T. K. Lee, E. Lee, S. Park, H. J. Lee, H. Jin, D. W. Lee, M.-G. Jeong, H.-G. Jung, K. Im, C. Hu, H. C. Ham, K. H. Song, Y.-E. Sung, Y. M. Lee, S. J. Yoo, *Energy Environ. Sci.* **2023**, *16*, 5019.